Improving Varifocal Mirror Performance Using Resonant Acoustic Chambers

LUIS RAYAS B3TJ1014

Department of Mechanical and Aerospace Engineering, Tohoku University

Academic Advisor: Professor Kazuhiro Hane

Abstract

Varifocal mirrors, useful in a variety of laser and optics applications, typically suffer performance loses from surrounding air and are usually vacuum packaged for this reason. Vacuum packaging is a non-negligible cost in the mass production of these devices. The varifocal mirrors considered in this paper are a class of common varifocal mirror designs which are circular membranes acted on by a force located near the circumference. This type of design very much resembles a number of common acoustic devices including drum heads and speakers and therefore have a number of well established associated acoustical models.

In this paper, a novel application of resonant sound waves is used to counteract such loses. A resonance chamber is placed on the backside of the mirror, providing an assistive force to the mirror. A device array consisting of 18 varifocal mirrors is proposed as a testing ground for these effects. The entire device consists of two parts, namely the device wafer and the resonance chambers, each constructed separately. The device wafer, which contains the array of simple membrane mirrors, is constructed using well known and common production techniques on an SOI (Si/SiO2/Si) wafer. Each mirror is approximately 1mm in diameter. The actuation method is via electrostatic force which is produced from a voltage applied between the mirror and the handle Silicon layer. This actuation force is concentrated within 50μm of the circumference, leading to an approximately spherical shape away from the edges. The resonance chambers are made from 5mm thick TEMPAX glass. Although precise alignment was unnecessary for this work, a method to create a precise alignment between multiple mirrors and their resonance chambers is proposed. The chambers themselves are primarily created through careful drilling of the TEMPAX glass with a standard diamond coated drill bit. In production, these two components could be bonded with the well known anodic bonding process, however for this work it was unnecessary. The theoretical aspects of sound resonance are used to estimate the expected improvement potentials. Given the scale of the device, chamber material and operating frequency the anticipated reflection efficiency is calculated to be nearly 100%; implying that nearly half of all losses to the air are recuperable (only one of the mirror sides is connected to a resonance chamber), implying a highly effective resonant effect. Finally, the response characteristics to an input voltage are analyzed using a scanning vibrometer.

Background

Varifocal mirrors in the under 1mm diameter range have been part of the research in MEMS technology since at least the 1970s. They are used in a number of optical technologies that use lasers at varying focal lengths. As with some other MEMS technologies, such mirrors suffer losses due to drag with the surrounding air and require vacuum packaging in order to perform at their desired specifications [1,2,3]. Vacuum packaging can add significantly to the cost of mass production of such devices [4] and as such there is room for improvement by either eliminating or diminishing these loses. Similar research has found limited success in CMUTs, another type of MEMS device, although the research also indicates potential, citing the device's incorrect tuning for its shortcomings [5].

Device Description and Design

The device consists of two distinct parts, the device layer which comprises the mirrors themselves and the chamber layer which contains cylindrical holes which act as the resonance chambers. The device wafer begins as an SOI wafer with a 200μm Si handle layer, a 600 nm Si02 BOX layer and finally a 2μm thick top Si layer. The wafer is 20 mm x 20 mm. The chamber block is also 20 mm x 20 mm with a height of 5 mm. The figures a-l in Fig. 1 show the process diagram for both the device wafer and chamber layer. The table in Table 1 provides details for each process a-l. In general the design was determined primarily by a desire for simplicity. The entire process requires only 3 masks and relies on simple tested manufacturing procedures.

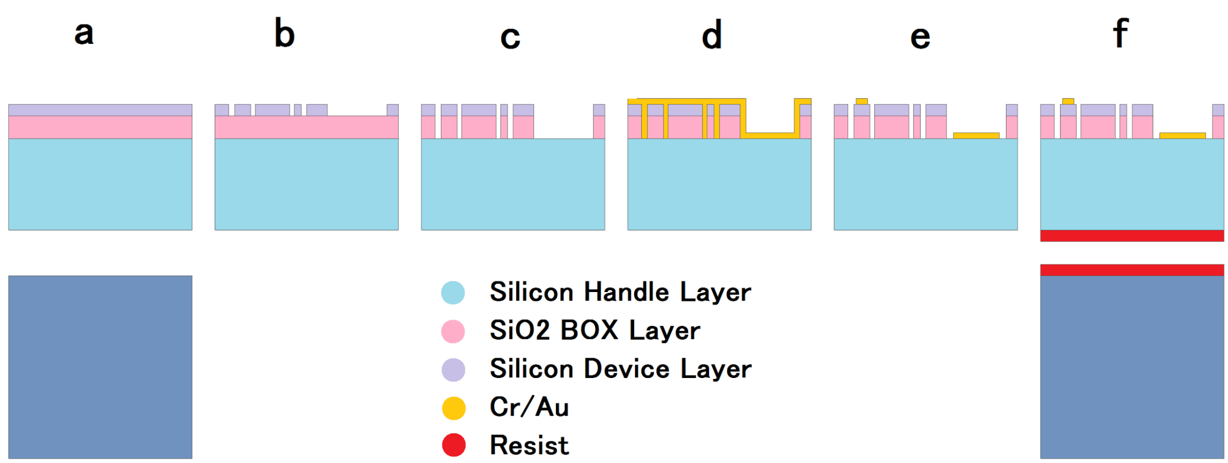

Figure 1a. Process diagram

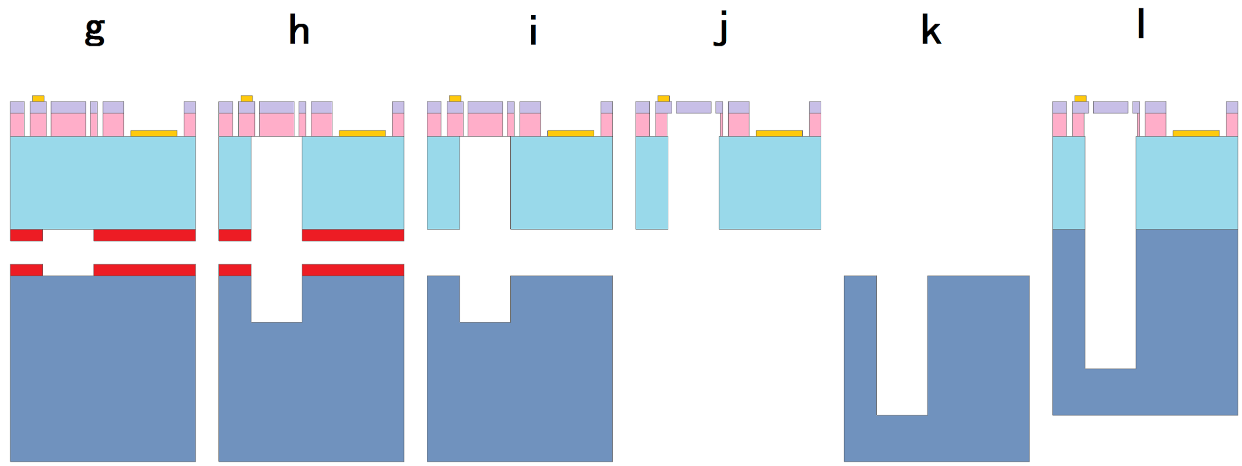

Figure 1b. Process diagram

a: Wafers	SOI (200, .6, 2)	TEMPAX (5mm)	N/A
b: Si Etching	create mirror pattern on top silicon	N/A	Mask 1, DRIE etching
c: SiO2 Etching	expose handle layer near electrical lead	N/A	LAL1000
d: Cr/Au Deposit	deposit a 50 nm layer of Cr then 200 nm of Au	N/A	50 nm/200 nm
e: Cr/Au Etching	etching pattern on metal contacts	N/A	Mask 2
f: Resist Deposit	backside	[proposed]	OFPR 800 200 cp
g: Resist Pattern	backside alignment	[proposed]	
h: Etching	etch up to BOX layer, DRIE etching	[proposed] etch as much as possible without absurd side etching (~15 microns), LAL1000	
i: Remove Resist			MS 2001
j: SiO2 Etching	expose mirror, side etch to expose electrode overlap	N/A	LAL1000

k: Drill Chamber	N/A	approximately 1.4 mm depth	diamond-coated 1 mm drill bit
l: Anodic Bonding	bond to chambers	bond to devices	[proposed]

Table 1. Process descriptions

Finally in Fig. 2 the mask designs are shown one atop another. The blue represents mask 1, orange mask 2, and green mask 3. The diameter of 1 mm was chosen because drill bits are much easier to find in this size than smaller sizes. 18 mirrors were put on the wafer for purposes of redundancy. Each mirror has its own metallic contact which maximizes the chance that a given mirror is well isolated from shorting.

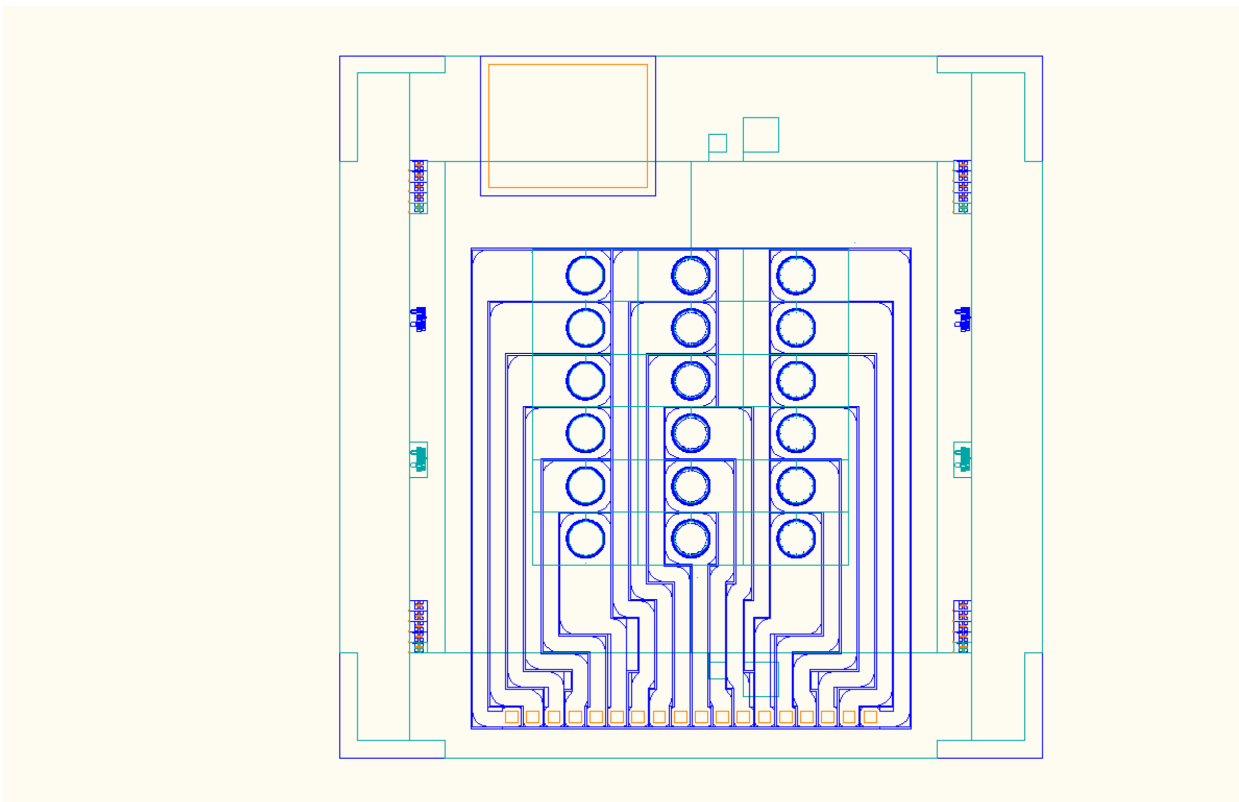

Figure 2. Mask designs. Blue - Mask 1 - Top Si, Orange - Mask 2 - Au/Cr, Green - Mask 3 - Handle Si

Theoretical Improvement Potential

A simplified approach to calculating the energy which can be regained will consider the energy lost at the boundary upon reflection. The effects of this interaction are determined by the impedances of the two materials by the following equation:

$$R = \frac{Z_2 - Z_1}{Z_2 + Z_1}$$

Where R is the reflection coefficient, which is simply the portion of the incident sound wave is reflected. In our case, Z_1 is the acoustic impedance of air, which is approximately 400 Rayls and Z_2 is the acoustic impedance of the TEMPAX borosilicate glass, approximately $1.3 * 10^7$ Rayls. The resultant value for R is approximately .99994. The energy reflected is related to the square of this value or about .99988.

The above calculation is useful to show a good choice in material however it is not sufficient as there are a number of other effects which may affect the efficiency of the reflection as well. Considering the shape of the propagation of a sound wave over directionality [6]:

$$P \approx C * (1 - (k * a * sin(\theta))^2/8)$$

Where a is the radius of the membrane and k is 2*pi*f/c we can calculate that the coefficient on sin:

$$.0005m * 2 * \pi * 58000Hz/(343m/s) = .53$$

does not create sidelobes (ka should be in the vicinity of 8 or greater for this to occur) and in fact is quite close to uniform directionality. This tells us that there should not be any significant losses due to poor scaling of relative sizes. In other words the dimensionless values for this device are in a good range. Ultimately there may be promise in following a thorough analysis of the theoretical losses that could yield a fairly accurate value for expectation improvement using work such as that in [7].

Results

The constructed device is shown in Fig. 3 during testing without the chambers and in Fig. 4 with the chambers. The profile of one of the mirrors is shown in Fig. 5.

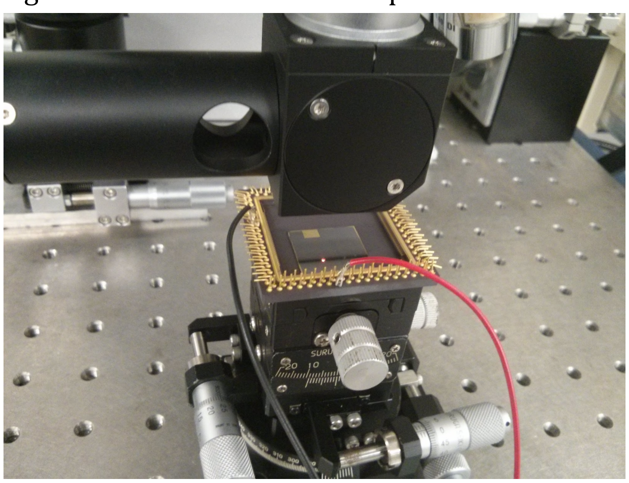

Figure 3. Complete device in testing without chambers

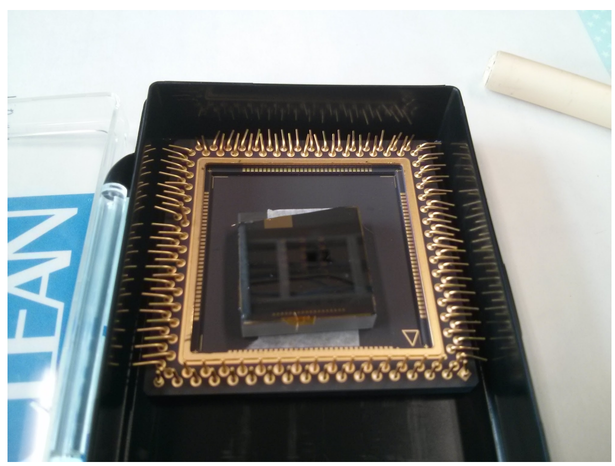

Figure 4. Device with chamber block attached

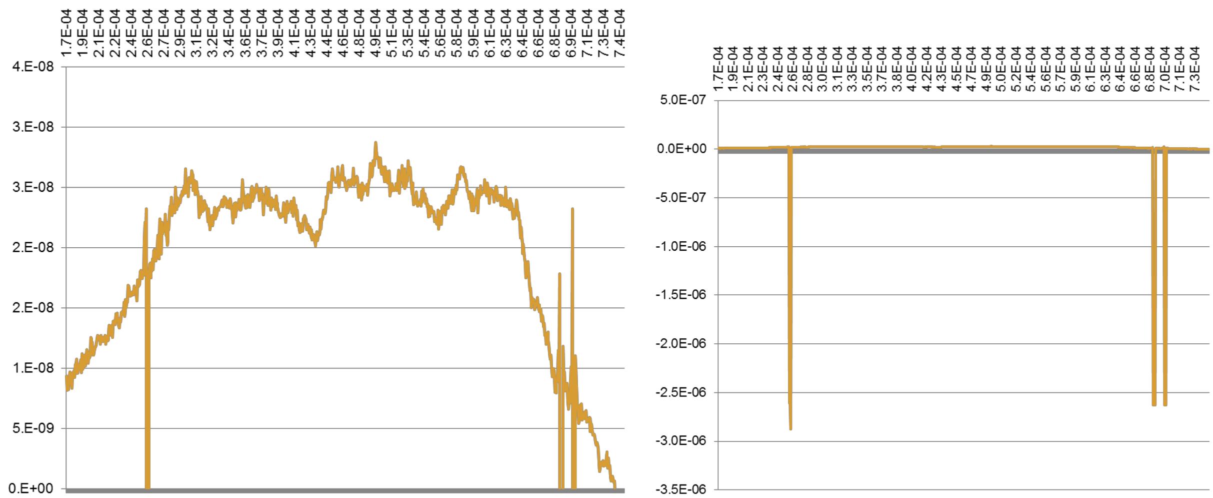

Figure 5 a,b. Mirror profile with no voltage applied. All units are meters.

Of the 18 mirrors, about half were "pulled in", meaning the device layer was stuck to the handle layer, an independent half had very noticeable defects and another 3 had minor defects. In the end 3 mirrors appeared to be without defects, one of which is shown in Fig. 6. Of these 3, one was shorted and one was confirmed to work as expected; this mirror was used in all of the following results.

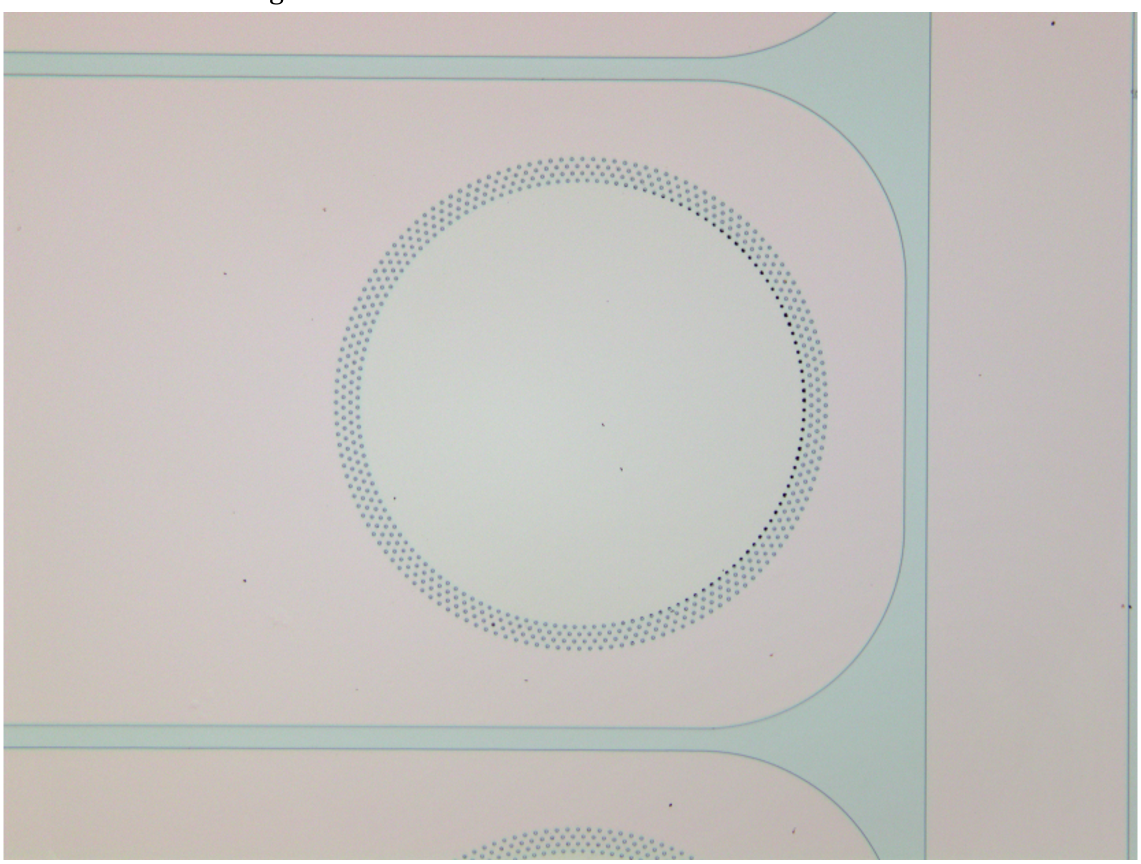

Figure 6. Photograph of a mirror without defects. Minor misalignment can be seen toward the right.

We use a scanning vibrometer to analyze the response of the mirror to an input signal. First, in order to estimate the necessary hole depth for the chambers as to get agreement between its inherent resonance frequency and the chambers', the mirror was tested alone. In this case we manually scanned the frequencies for the best response on the FFT transform performed by the vibrometer. We found approximately 58.4 kHz to respond best. The output of the vibrometer when inputting this frequency is shown in [xxxfig]. From this, the calculation to estimate the optimal depth for the chambers is simple. Using 343 m/s for the speed of sound in air:

$$d = \lambda/4 = \frac{v}{4f} = 343/4/58400 \approx 1.47mm$$

The holes were drilled to approximately 1.2 mm in depth, leaving .2 for the thickness of the handle layer and .07 mm for the thickness of the double-sided tape used in the assembly.

After attaching the chambers to the back of the device wafer the same test was performed on the same mirror, the results are shown in Fig. 7 and can be compared to Fig. 8. The comparison shows an approximately 20 times increase in the magnitude of oscillation, a promising but somewhat suspiciously successful result. More thorough testing without the resonant chambers is required before this numerical result should be taken at face value.

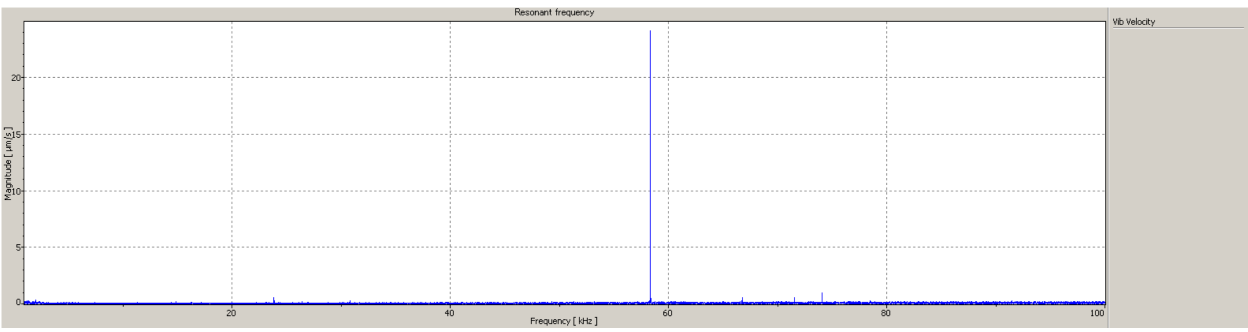

Figure 7. Frequency response when supplied 58360 Hz 10V amplitude signal. No chambers.

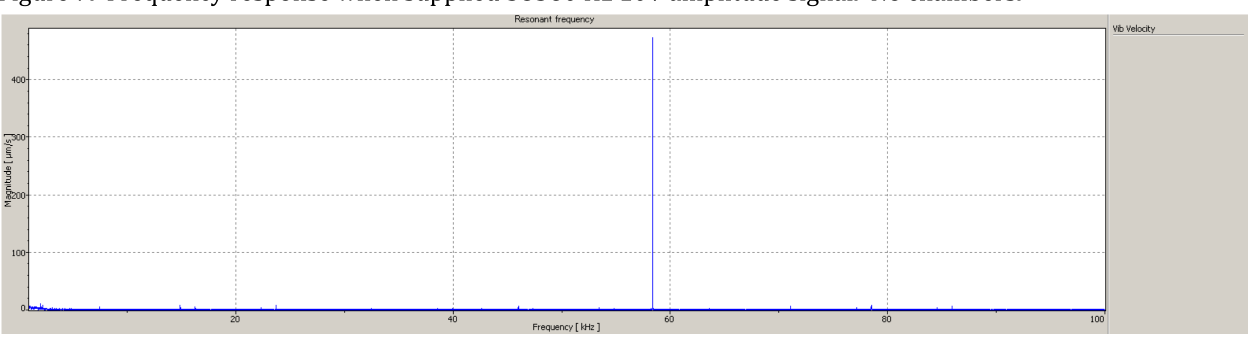

Figure 8. Frequency response of the same mirror at 58360 Hz 10V signal with resonant chambers.

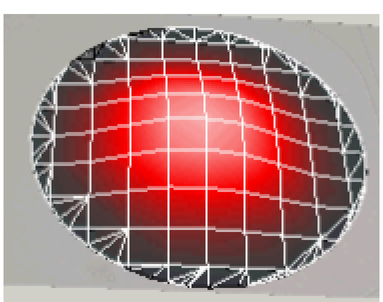

Finally, a full scan across the mirror's area and across frequencies was performed. Due to limitations of the setup, this experiment necessitated being done using an input amplitude of 3V. The results can be seen in Fig. 9 and to the left. From this scan we see that in fact about 54 kHz is where the first mode is located. It is possible that the effect of the resonance is overpowering that of the mirror and the chamber has this resonance frequency of 54 kHz. More testing is required to determine whether this is the case or whether we simply misestimated the resonant frequency of the device without the resonant chamber in the first place. The next large peak in Fig. 9 corresponds to the 1-1 mode of the membrane.

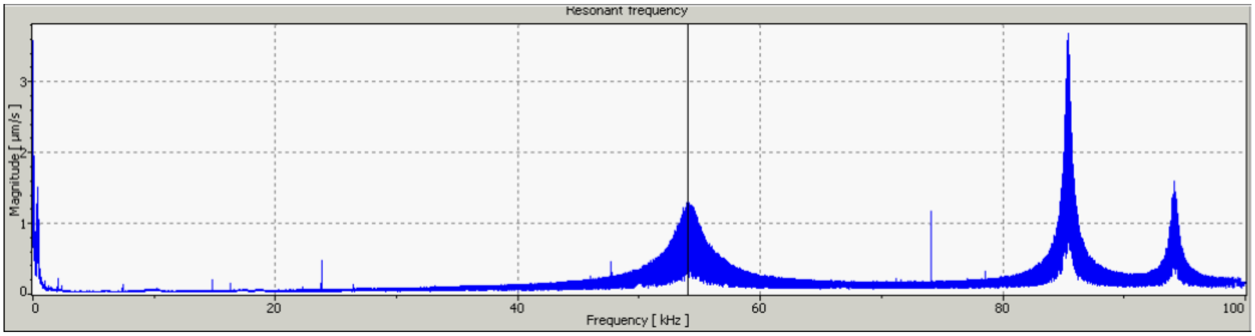

Figure 9. Frequency scan of the device's response with 3V amplitude input.

Conclusion

A device ideal for testing potentials in using acoustic energy as a source of performance improvement is proposed and constructed. We find its resonant frequency to be somewhere between 54 kHz and 58 kHz. We proceed to show that the preliminary result suggests a 20 times increase in the devices oscillation amplitude, a high enough improvement to be suspicious. Although there are a number of avenues to improve this research it nonetheless shows great potential.

Among the potential improvements to the research thus far completed, a method for accurately drilling holes of such depth was not ultimately found. The required depth being greater than 1 mm excludes traditional MEMS methods. Drills are effective but resource limitations excluded a drill with fine tuned depth control. Furthermore, drills necessarily leave a rough surface, which can be a negative for sound propagation.

Perhaps the most immediately valuable future improvement is thorough testing of the device without the chambers backing. A frequency scan should be performed and as much as possible the entire mirror excluding resonant chambers ought to be characterized.

Finally, we believe theoretical justification for the quantitative results can be obtained to a fairly good degree of accuracy, providing a better understanding of the underlying mechanism. Applying the methods in [7] to this problem would be a good place to start.

Acknowledgements

I would like to thank Mr. Kenta Nakazawa and Mr. Takashi Sasaki for the enormous amount of assistance received from them in the production and testing of this device.

References

1. U. Hofmann, M. Aikio; Biaxial Tripod MEMS Mirror and Omnidirectional Lens for a Low Cost Wide Angle Laser Range Sensor; http://link.springer.com/chapter/10.1007%2F978-3-642-29673-4_30

2. U. Hofmann; MEMS mirror for low cost laser scanners; http://www.minifaros.eu/data/AMAA_Minifaros_c_02_ulrich-hofmann_Fraunhofer_presentation.pdf

3. T. Sasaki, D. Sato, K. Hane; Displacement-amplified dynamic varifocal mirror using mechanical resonance; http://ieeexplore.ieee.org/xpls/icp.jsp?arnumber=6659109

4. R. Gooch, T. Schimert; Low-Cost Wafer-Level Vacuum Packaging for MEMS; http://journals.cambridge.org/download.php?file=%2FMRS%2FMRS28_01%2FS0883769400017310a.pdf&code=825fcf5be52dcb21329e7a33e0a9df0e

5. A. O. Manzanares, F. Montero de Espinosa; Air-coupled MUMPs capacitive micromachined ultrasonic transducers with resonant cavities; http://www.sciencedirect.com/science/article/pii/S0041624X11002423

6. D. Russell; Radiation from a Baffled Piston (model for a loudspeaker); http://www.acs.psu.edu/drussell/demos/baffledpiston/baffledpiston.html

7. Y. Ilinskii, B. Lipkens, E. A. Zabolotskaya; Energy losses in an acoustical resonator; http://www.zainea.com/bart.pdf